

Rotational Bands in ^{168}Tm from the $^{169}\text{Tm}(d, t)^{168}\text{Tm}$ Reaction*

J. J. Kolata† and J. V. Maher

Nuclear Physics Laboratory, University of Pittsburgh, Pittsburgh, Pennsylvania 15213

(Received 5 March 1973)

The $^{169}\text{Tm}(d, t)^{168}\text{Tm}$ reaction has been studied at an incident deuteron energy of 17.0 MeV. The excitation energies of more than 55 states up to 1.5 MeV in the residual nucleus were obtained to an accuracy of $\pm 0.15\%$, and the ground-state Q value for the $^{169}\text{Tm}(d, t)^{168}\text{Tm}$ reaction was measured to be $Q_0 = -1775 \pm 6$ keV. Differential cross sections were measured at 2.5° intervals from $7.5^\circ \leq \theta_{\text{lab}} \leq 45^\circ$, and then at 5° intervals for $45^\circ \leq \theta_{\text{lab}} \leq 90^\circ$ for most of these transitions. The resulting angular distributions were found to be well described by distorted-wave calculations for almost all transitions observed. The l -transfer values deduced for these transitions allowed the assignment of a narrow range of J^π values to the corresponding states in ^{168}Tm , independent of arguments based on the Nilsson-model predictions of transition strengths. Several anomalous angular distributions to presumably well-known rotational states which apparently cannot be explained by the distorted-wave calculations are discussed. Spectroscopic factors for all the observed transitions were computed and are compared to the Nilsson-model predictions for low-lying negative-parity bands. Transition-strength anomalies are discussed.

I. INTRODUCTION

In common with the other rare-earth isotopes in this mass region ^{168}Tm is a permanently deformed system, so that its low-energy spectrum is expected to consist of "intrinsic" states, formed by the coupling of the valence nucleons, with superimposed rotational bands.¹ The energies of these states and their single-neutron-transfer spectroscopic factors are usually predicted using Nilsson-model wave functions for the deformed single-particle orbitals. The distorted-wave Born approximation (DWBA) is frequently used to treat the reaction mechanism.² However, serious questions have been raised about the adequacy of conventional DWBA calculations as applied to these deformed systems. Theoretical studies have indicated a need for scattering wave functions (representing both incoming and outgoing systems) which include effects due to inelastic excitations³ and for more realistic form factors representing the neutron bound-state wave function.⁴ Complementary experimental work⁵ has shown a strong dependence on optical-model parameter values in several cases. Previous investigations of (d, t) reactions on deformed nuclei⁶ have tended to be performed at incident beam energies quite close to the Coulomb barrier and data are typically taken at only two or three angles. Complete angular distributions taken at higher-beam energies allow model-independent determination of orbital angular momentum transfer (l) and thus might be expected to shed some light on these reaction mechanism questions. As a first step in a survey of single-neutron-transfer reactions on well-de-

formed rare-earth targets, we have studied the odd-odd nucleus ^{168}Tm with 17-MeV deuterons. As is discussed below, this deuteron energy has proved to be high enough that angular distribution shapes are strongly characteristic of orbital angular momentum transfer. The availability of data such as are presented herein should be of use for further theoretical studies of the kind discussed above. However, improved reaction mechanism codes are not generally available and for this reason the results presented below are analyzed and discussed in terms of a standard distorted-wave Born-approximation treatment.

As recently as 1971, very little experimental information on ^{168}Tm was available. Since then an investigation of the $^{169}\text{Tm}(d, t)^{168}\text{Tm}$ reaction by Jones and Sheline⁷ has been published, and additional as yet unpublished work has been done on the (d, t) ⁸ and $(^3\text{He}, d)$, (α, t) , $(^3\text{He}, \alpha)$, and (d, t) reactions⁹ to states in ^{168}Tm . Except for the preliminary account of the present work,⁸ no angular distributions were obtained in these studies so that the spins and parity assignments proposed for excited states of ^{168}Tm were based on Nilsson-model predictions for the excitation energies of and the intensity patterns to the rotational states.^{7,9} In the present experiment, we have obtained accurate excitation energies and narrow J^π limits for most of the states up to 1.5 MeV in ^{168}Tm populated in the $^{169}\text{Tm}(d, t)$ reaction. In Sec. IV A, the spin-parity limits extracted from the angular distributions are compared with previous suggestions,^{7,9} and additional assignments are proposed for some of the low-lying states. Finally, some anomalies in certain angular distributions and

spectroscopic factors are discussed in Secs. IV B and C.

II. EXPERIMENTAL METHOD

The $^{169}\text{Tm}(d, t)^{168}\text{Tm}$ reaction was performed with a 17.0-MeV deuteron beam from the University of Pittsburgh three-stage Van de Graaff accelerator. This beam was focused through a 0.5-mm-wide by 2-mm-high collimating aperture (followed by an antiscattering slit) placed about 2 cm from the target position in the scattering chamber. The maximum angular divergence of the incident beam was less than $\pm 0.5^\circ$. The incident beam was continuously monitored by two NaI(Tl) scintillators at $\pm 38^\circ$ relative to the beam direction. Deuterons elastically scattered into these counters, as well as the charge collected in a Faraday cup, were used to normalize the relative differential cross sections at the various angles.

The targets were typically $100\text{-}\mu\text{g}/\text{cm}^2$ films of natural ^{169}Tm metal evaporated onto $20\text{-}\mu\text{g}/\text{cm}^2$ C backings. Target thickness was determined by measuring the Rutherford scattering of 10.0-MeV deuterons into the monitor counters, and also by comparing the elastic scattering of 17.0-MeV deuterons into the monitor detectors with optical-model predictions using standard parameters discussed below. The estimated uncertainty in the absolute cross sections is less than $\pm 25\%$.

The reaction tritons were detected in $50\text{-}\mu\text{m}$ Kodak NTB nuclear emulsions placed in the focal plane of an Enge split-pole spectrograph. A typ-

ical spectrum is shown in Fig. 1. Major contributions to the experimental energy resolution come from beam spot size and divergence (7 keV), differential energy loss and straggling in the target (3 keV), beam energy spread and spectrograph aberrations (3 keV), and plate-scanning resolution (3 keV). These factors account entirely for the total experimental energy resolution of 9-keV full width at half maximum (FWHM).

Differential cross sections were measured at 2.5° intervals from 7.5 to 45° in the laboratory system, and then at 5° intervals from 45 to 90° . Most of the spectra obtained were analyzed using the program AUTOFIT¹⁰ with numerous hand checks to ensure the reliability of the fitting procedure.

As is discussed below, there is evidence that the ^{168}Tm ground state is not appreciably populated in the (d, t) reaction and that the first state seen in this experiment has an excitation energy of ~ 5 keV. Since the exact value of the (small) excitation energy of the first state seen in this work is not well determined, all excitation energies quoted for states populated in this experiment will be relative to the energy of that first state. Within the framework of this qualification, accurate excitation energies for states in ^{168}Tm observed in this experiment were obtained by direct comparison¹¹ to the states of ^{207}Pb excited in the $^{208}\text{Pb}(d, t)\text{-}^{207}\text{Pb}$ reaction. The two (d, t) reactions were observed on the same photographic plate, with the incident beam energy, spectrograph laboratory angle, magnetic field setting, and focal-plane ad-

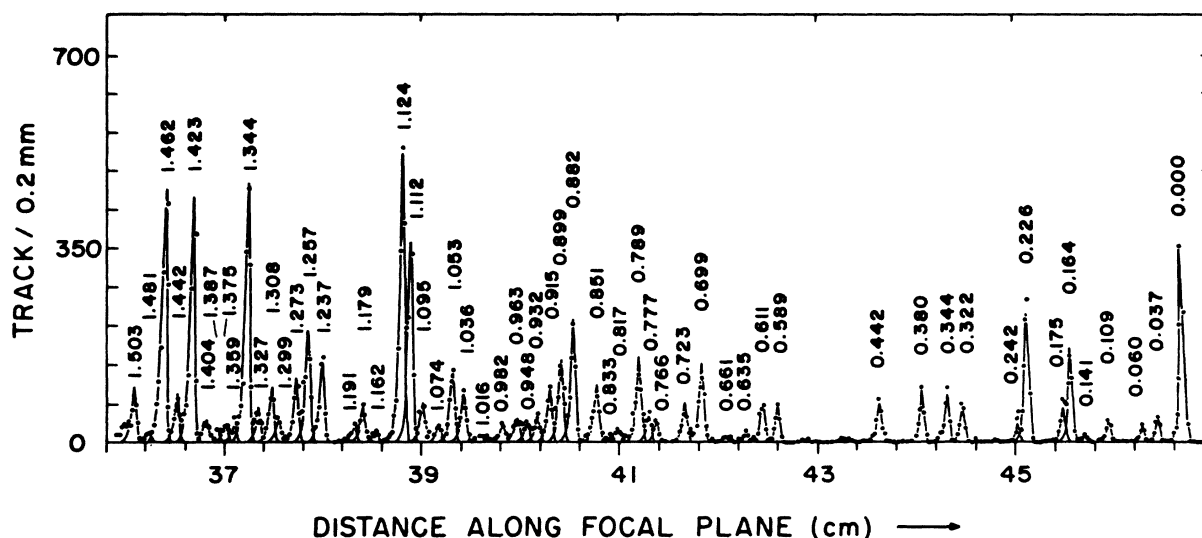


FIG. 1. Typical spectrum for the $^{169}\text{Tm}(d, t)^{168}\text{Tm}$ reaction. The curves drawn through the data points were generated by the AUTOFIT code using a standard peak shape determined from the transition to the state at 0.0 keV. Excitation energies for the ^{168}Tm triton groups are labeled in MeV, relative to the state at 0.0 keV. Note that this state may not in fact be the ground state (see the text for a discussion of this point).

justment held fixed. The dominant contribution to excitation-energy errors is then the rms uncertainty in the ^{168}Tm peak centroids, since the ^{207}Pb standard spectrum energies are very well known.¹² This reference spectrum method was also used to extract an accurate ground-state Q value for the $^{168}\text{Tm}(d, t)^{168}\text{Tm}$ reaction.

III. RESULTS

The excitation energies determined in this experiment are listed in Table I. Unless otherwise indicated, they are believed to be accurate to ± 1.5 keV or $\pm 0.15\%$ (whichever is greater). However, several of the states listed in Table I have larger assigned errors, reflecting larger rms deviations in excitation-energy measurements at the various angles for which data were taken. The present results are in agreement with those of Ref. 7 for states in the first 0.5 MeV of excitation, but there

is a systematic discrepancy for states above this energy which reaches 8 keV at 1.5 MeV. The error estimates of Ref. 7, however, do not include an evaluation of possible systematic errors and are based only on the rms spread in excitation energy obtained in three separate exposures. The errors we quote here include an estimate of possible systematic scale errors in the reference spectrum calibration. The excitation energies listed in Table I do not agree with preliminary results from the $(^3\text{He}, \alpha)$ experiment quoted in Ref. 9. These data suggest that the actual ground state is about 5 keV below the lowest state observed in the (d, t) reaction.⁹ We find that the Q value for this lowest observed state of ^{168}Tm is -669 ± 5 keV relative to the ground state of ^{207}Pb in the reference spectrum. Using the known Q value for the $^{208}\text{Pb}(d, t)^{207}\text{Pb}$ reaction,¹³ we compute $Q = -1780 \pm 6$ keV for this state. Since the actual ground state is 5 keV lower, the ground-state Q value for the $^{168}\text{Tm}(d, t)$

TABLE I. Experimental excitation energies, l -transfer values, and spectroscopic factors for $^{168}\text{Tm}(d, t)^{168}\text{Tm}$. Unless otherwise indicated, the excitation energies are accurate to ± 1.5 keV or $\pm 0.15\%$ (whichever is greater), and are quoted relative to level 0. Note that this level may not in fact be the ground state (see the text for further discussion of this point). The quoted errors include statistical uncertainties in the peak positions, and also an estimate of systematic errors introduced in separating close-lying doublets and in the calibration procedure. The last column lists spin and parity limits deduced from the experimental angular distributions. Less certain values are enclosed in parentheses.

Level	E_x (MeV)	$l_{(d, t)}$	C^2S	J^π limits	Level	E_x (MeV)	$l_{(d, t)}$	C^2S	J^π limits
0	0.000	1	0.14	0 ⁻ 2 ⁻	30	0.963 ± 3	(3 + 5)	(0.05 + 0.52)	(4 ⁻)
1	0.037	(3)	(0.04)	(2 ⁻ 4 ⁻)	31	0.982 ± 2	3	0.055	2 ⁻ 4 ⁻
2	0.060	4	0.30	3 ⁺ 5 ⁺	32	1.016 ± 6	(3)	(0.03)	(2 ⁻ 4 ⁻)
3	0.109	(3)	(0.04)	(2 ⁻ 4 ⁻)	33	1.036	3	0.17	2 ⁻ 4 ⁻
4	0.141 ± 3	4	0.14	3 ⁺ 5 ⁺	34	1.053	3	0.24	2 ⁻ 4 ⁻
5	0.164 ± 2	1	0.084	0 ⁻ 2 ⁻	35	1.074 ± 5	(3)	(0.07)	(2 ⁻ 4 ⁻)
6	0.175 ± 2	(3)	(0.07)	(2 ⁻ 4 ⁻)	36	1.095	(5)	(1.6)	(4 ⁻ 6 ⁻)
7	0.226	1	0.11	0 ⁻ 2 ⁻	37	1.112	2	0.58	1 ⁺ 3 ⁺
8	0.242 ± 6	6	1.25	5 ⁺ 7 ⁺	38	1.124	0	0.27	0 ⁺ 1 ⁺
9	0.322	(3)	(0.09)	(2 ⁻ 4 ⁻)	39	1.162 ± 2	(5)	(0.54)	(4 ⁻ 6 ⁻)
10	0.344	3	0.12	2 ⁻ 4 ⁻	40	1.179	(2)	(0.10)	(1 ⁺ 3 ⁺)
11	0.380	3	0.11	2 ⁻ 4 ⁻	41	1.191 ± 2	(2)	(0.05)	(1 ⁺ 3 ⁺)
12	0.442 ± 2	6	1.5	5 ⁺ 7 ⁺	42	1.237	2	0.23	1 ⁺ 3 ⁺
13	0.589	3	0.09	2 ⁻ 4 ⁻	43	1.257	2	0.35	1 ⁺ 3 ⁺
14	0.611 ± 2	1	0.029	0 ⁻ 2 ⁻	44	1.273	2	0.22	1 ⁺ 3 ⁺
15	0.635 ± 2	1	0.009	0 ⁻ 2 ⁻	45	1.299	(2)	(0.09)	(1 ⁺ 3 ⁺)
16	0.661 ± 2	1	0.007	0 ⁻ 2 ⁻	46	1.308	0	0.048	0 ⁺ 1 ⁺
17	0.699 ± 2	(1 + 3)	(0.05 + 0.11)	(2 ⁻)	47	1.327	(3)	(0.15)	(2 ⁻ 4 ⁻)
18	0.723	3	0.12	2 ⁻ 4 ⁻	48	1.344	0	0.28	0 ⁺ 1 ⁺
19	0.766 ± 2	(4)	(0.62)	(3 ⁺ 5 ⁺)	49	1.359 ± 2	(2)	(0.09)	(1 ⁺ 3 ⁺)
20	0.777 ± 3	(1 + 3)	(0.01 + 0.05)	(2 ⁻)	50	1.375 ± 3	(2)	(0.08)	(1 ⁺ 3 ⁺)
21	0.789	1	0.057	0 ⁻ 2 ⁻	51	1.387 ± 6	(1)	0.016	(0 ⁻ 2 ⁻)
22	0.817 ± 2	(2)	(0.04)	(1 ⁺ 3 ⁺)	52	1.404 ± 4	0	0.035	0 ⁺ 1 ⁺
23	0.833 ± 4	1	0.009	0 ⁻ 2 ⁻	53	1.423	0	0.27	0 ⁺ 1 ⁺
24	0.851 ± 2	3	0.18	2 ⁻ 4 ⁻	54	1.442	0	0.051	0 ⁺ 1 ⁺
25	0.882	1	0.10	0 ⁻ 2 ⁻	55	1.462	0	0.28	0 ⁺ 1 ⁺
26	0.899	(1 + 3)	(0.06 + 0.08)	(2 ⁻)	56	1.481 ± 5	(2)	(0.05)	(1 ⁺ 3 ⁺)
27	0.915	(3 + 5)	(0.09 + 1.2)	(4 ⁻)	57	1.503 ± 2	0	0.068	0 ⁺ 1 ⁺
28	0.932	3	0.10	2 ⁻ 4 ⁻					
29	0.948 ± 3	3	0.081	2 ⁻ 4 ⁻					

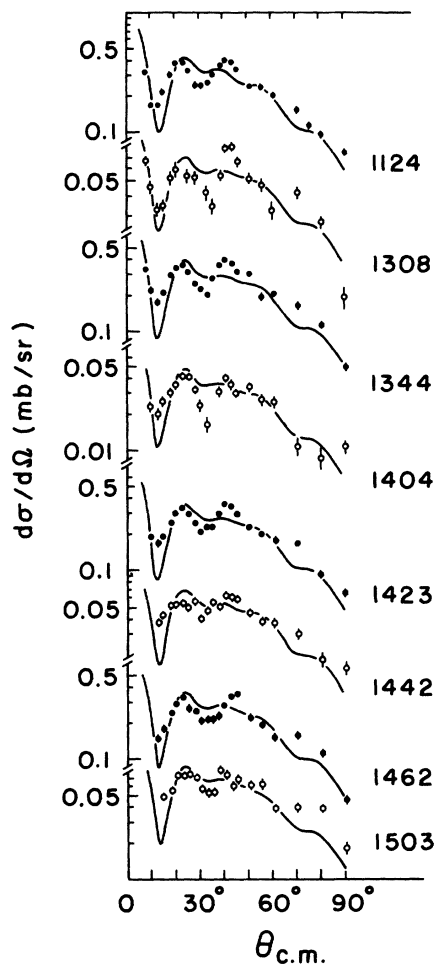


FIG. 2. Experimental angular distributions for $l=0$ transitions. Error bars include statistical errors and also an estimate of errors in background subtraction and in the separation of close-lying states. The solid curves are $l=0$ DWBA calculations.

^{168}Tm reaction is $Q_0 = -1775 \pm 6$ keV.

The angular distributions obtained for transitions to 58 states in ^{168}Tm below 1.5 MeV of excitation are shown in Figs. 2–8. The error bars are primarily statistical (standard deviation), but include an estimate of errors in background subtraction for weak peaks and in the separation of close-lying doublets. The uncertainty in the relative normalization (< 5%) is the dominant error for the strongest groups. The curves shown in Figs. 2–8 were computed in the distorted-wave Born approximation using the code DWUCK¹⁴ with optical-model parameters listed in Table II. Finite range and nonlocality corrections (in the local energy approximation¹⁵) were included. The range parameter was 0.845. Nonlocality parameters were: $\beta_d = 0.54$, $\beta_t = 0.25$. Nonlocality corrections were not applied to the bound-state form factor. The bound-state

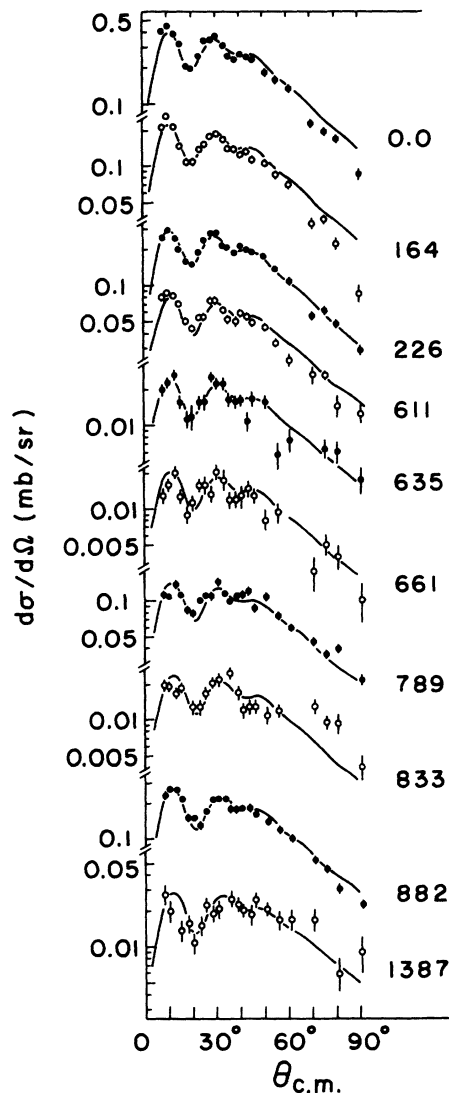


FIG. 3. Comparison of $^{169}\text{Tm}(d,t)^{168}\text{Tm}$ data with $l=1$ DWBA calculations. Experimental error bars include statistics and background uncertainties.

wave functions were obtained by binding a neutron in a Woods-Saxon well with parameters listed in Table II and adjusting the well depth to fit the empirical neutron separation energy for the state in question. The (spherical) shell-model orbital for a given angular momentum assumed in these calculations was the one nearest the Fermi surface for a spherical configuration of 100 neutrons (see Table III). The problems associated with this inconsistent use of spherical single-particle wave functions to describe deformed systems have been well documented^{16, 17} and will be discussed in more detail below.

Since ^{169}Tm , the target nucleus for this experiment, has a ground-state spin $J = \frac{1}{2}$, two l -trans-

TABLE II. Optical-model parameters used in the distorted-wave calculations. Also listed are the bound-state well parameters.

	V (MeV)	r_0 (fm)	r_c (fm)	a (fm)	W (MeV)	W_D (MeV)	r_I (fm)	a_I (fm)	λ_{s_0}
$^{169}\text{Tm} + d^a$	107.0	1.15	1.15	0.81	...	17.6	1.34	0.68	...
$^{168}\text{Tm} + t^b$	166.7	1.16	1.40	0.752	14.7	...	1.498	0.817	...
Bound states	c	1.17	1.17	0.75					25.0

^a C. M. Perey and F. G. Perey, Phys. Rev. **132**, 755 (1963).

^b E. R. Flynn, D. D. Armstrong, J. G. Beery, and A. G. Blair, Phys. Rev. **182**, 1113 (1969).

^c Adjusted to give correct separation energy.

fer values are generally possible in the (d, t) transition to a given final state in ^{168}Tm . The Nilsson model, however, predicts that most of the stronger transitions should be dominated by a single l transfer, which is usually the lowest value permitted for a given final state. This lower l value is also favored by the kinematics of the (d, t) reaction at 17.0 MeV. That is, the DWBA cross section is largest (for unit spectroscopic factor) for $l=0$ and $l=1$ transitions. If a direct-

reaction mechanism predominates, we might expect to see angular distributions which are characteristic of each l -transfer value and are also reasonably well described by the DWBA. This expectation is for the most part borne out by the present data (Figs. 2-7). Only a minority of the experimental angular distributions cannot be acceptably fitted with a unique l value, and several of these are easily interpretable in terms of appropriate mixtures of l -transfer values (Fig. 8). Neutron l -transfer values obtained by comparison to DWBA predictions are listed in Table I for all transitions observed, along with the J^π limits deduced from them. These parity assignments and spin limits are in good agreement with previous suggestions^{7,9} for states below 600 keV, except for the 226-keV state which is assigned 5^+ in Ref. 9 and $(0-2)^-$ here. It is possible, of course, that the (d, t) and $(^3\text{He}, \alpha)$ reactions are populating two different unresolved states. However, the spin suggestions of Ref. 9 are partly based on a comparison of the (d, t) and $(^3\text{He}, \alpha)$ cross sections to this state. This cross-section ratio would be very difficult to estimate if the state were a doublet, particularly in view of the fact that we see no evidence for a high angular momentum component

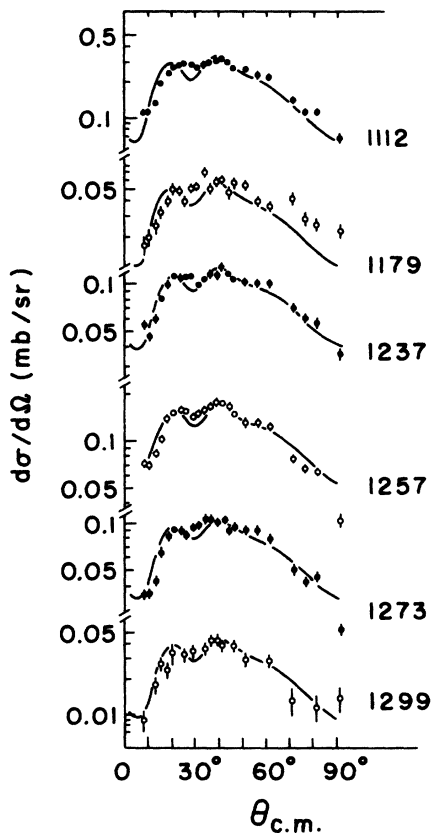


FIG. 4. Angular distributions for $l=2$ transitions compared with the DWBA calculations. Experimental error bars include statistics and background uncertainties. Where they are not shown, the error bars are smaller than the points.

TABLE III. Spherical shell-model orbitals assumed for the bound neutron in the distorted-wave calculations. In this convention, the lowest orbital is labeled $1s_{1/2}$. Note that calculations were performed for both the $d_{3/2}$ and $d_{5/2}$ states.

n	l	j
3	s	$\frac{1}{2}$
3	p	$\frac{3}{2}$
2	d	$\frac{3}{2}$
2	d	$\frac{5}{2}$
2	f	$\frac{7}{2}$
1	g	$\frac{7}{2}$
1	h	$\frac{9}{2}$
1	i	$\frac{11}{2}$

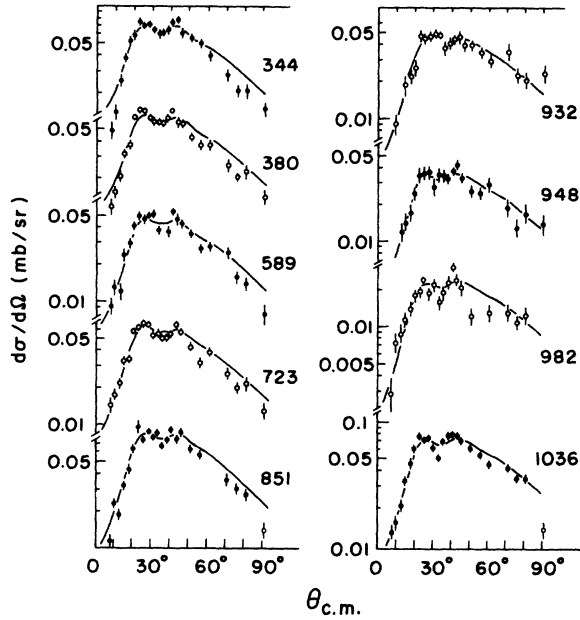


FIG. 5. Angular distributions for $l=3$ transitions compared with DWBA calculations. Where they are not shown, the error bars are smaller than the points.

in the (d, t) angular distribution at 17 MeV (Fig. 3). No spin-parity suggestions have previously been made for states above 600 keV of excitation energy to compare with the J^π limits for those levels given in Table I.

Spectroscopic factors for all transitions studied were computed by comparing the cross-section predictions of the DWBA theory to the experimental absolute differential cross sections. The formula used was:

$$\left(\frac{d\sigma}{d\Omega}\right)_{\text{exp}} = 3.33 \sum_l (C^2S)_l \frac{1}{2j+1} \left(\frac{d\sigma}{d\Omega}\right)_{\text{DWBA}, l},$$

where j is the assumed angular momentum transfer. Although the shapes of the predicted angular distributions are not strongly Q value dependent, this was not the case for their magnitudes. Therefore, complete calculations were performed for each l value at 500-keV intervals in excitation energy. The Q dependence was found to be nearly the same for all l values. It was well represented by the expression:

$$\sigma(E_x) = \sigma(E_x=0) e^{-0.34E_x - 0.11E_x^2},$$

where E_x is the excitation energy relative to the ground state and $\sigma(E_x=0)$ is the total DWBA cross section to the state in question if it was the ground state. The resulting neutron-transfer cross sections were interpolated to the appropriate Q value using this formula. The spectroscopic factors

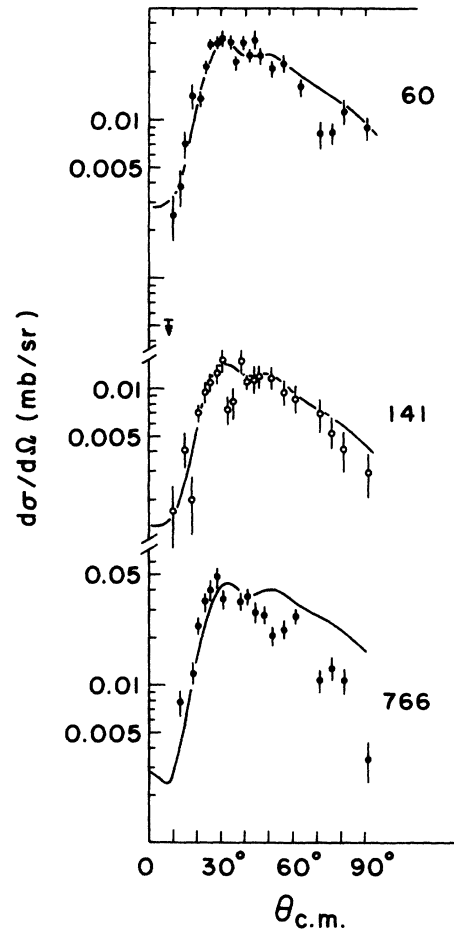


FIG. 6. Angular distributions for $l=4$ transitions compared with DWBA calculations. The arrow on the 7.5° data point for the transition to the 60-keV level indicates an upper bound to the cross section. Where they are not shown, the error bars are smaller than the points.

computed in this manner are listed in Table I for all transitions observed in this work.

IV. DISCUSSION

A. Spectroscopic Information

1. Ground Band

The two-quasiparticle states of ^{168}Tm populated in the direct (d, t) reaction should be formed by coupling an odd proton in the $[411]_{\frac{1}{2}}^+$ Nilsson orbital to the neutron-hole states of the $N=100$ system. The spectroscopy of low-lying single-particle levels in the neighboring odd- A isotones ^{167}Er and ^{168}Yb is known from studies of (d, p) , (d, t) , and (n, γ) reactions.^{2, 18, 19} In both of these nuclei, the $[633]_{\frac{7}{2}}^+$ neutron hole is the ground state, the first excited quasiparticle state being the $[521]_{\frac{1}{2}}^-$ neutron orbital at 208 keV in ^{167}Er and 24 keV in ^{168}Yb . Therefore, the ground state of

^{168}Tm should result from the coupling of the $[411]_{\frac{1}{2}^+}$ proton and the $[633]_{\frac{7}{2}^+}$ neutron hole, which yields two positive-parity bands with $K=3$ and $K=4$ depending on the relative orientation of the odd-nucleon spin vectors.²⁰ The Gallagher-Moszkowski rule²¹ suggests that the $K^\pi=3^+$ band will be the ground band in this case. The Nilsson model predicts a very weak transition to the 3^+ band head which we have not seen in the present experiment. Preibisz and Burke⁹ have identified the ground-state transition in the $(^3\text{He}, \alpha)$ reaction for which the $l=1$ transition to the state 5 keV higher is not kinematically favored as in (d, t) .

The 4^+ , 5^+ , and 6^+ members of the $K=3$ rotational band have been previously identified with the states at 60, 141, and 242 keV respectively.^{7,9} The spin limits listed in Table I are in good agreement with these suggested assignments. The Nilsson model predicts a strong $l=4$ transition to the $(5^+, 3)$ state as observed.

We have not seen the transition to the 7^+ member of the ground-state band, which is expected to be weak. The level at 445 keV, however, is at about the expected position for the 7^+ member of the $K=4$ band.⁷ The spin limits for the state (Table I) are in agreement with this suggestion, and furthermore the Nilsson model predicts a weak $l=4$ transition to the $(5^+, 4)$ state and a very weak transition to the $(6^+, 4)$ state which are the other possible assignments for this level. It seems, then, that the $(7^+, 4)$ assignment is quite probably in agreement with the results of Ref. 9. On the other hand, the state at 226 keV is assigned to the 5^+ member of the $K=4$ band in Ref. 9, compared with the present 0 to 2 spin limit and negative-parity assignment. Possibly this state is a doublet with the 5^+ component being populated only in the $(^3\text{He}, \alpha)$ reaction. We see no evidence for a high l -transfer component in the (d, t) transition to this level (Fig. 3).

2. Levels Arising from the $[521]_{\frac{1}{2}^-}$ Neutron Orbital

Two negative-parity bands with $K=0$ and 1 can be formed from the $[411]_{\frac{1}{2}^+}$ and $[521]_{\frac{1}{2}^-}$ Nilsson states. In this case, the Gallagher-Moszkowski rule predicts that the $K^\pi=1^-$ band will be at a lower excitation energy. However, the rotational excitation energies for both bands will be greatly distorted by mutual Coriolis coupling. The Coriolis matrix element²² is a linear combination of terms containing the decoupling parameters of the two Nilsson orbitals, each of which has $|\Omega|=\frac{1}{2}$. Since the two decoupling parameters happen to be nearly equal in magnitude but of opposite sign,² the Coriolis matrix element almost vanishes for

odd- l states and is very large for even- l states (except for the 0^- band head which does not couple to any of the states in the $K^\pi=1^-$ band).

The states at 0.0, 37, 109, and 175 keV may be identified with the first four members of the $K^\pi=1^-$ band on the basis of the parity assignments and spin limits for these states listed in Table I. The strong $l=1$ transitions to the states at 164 and 226 keV suggest that these are the 0^- and 1^- members of the $K=0$ band, respectively. The Nilsson model predicts a very weak, mixed $l=1+3$ transition to the $(2^-, 0)$ state which we do not see in the

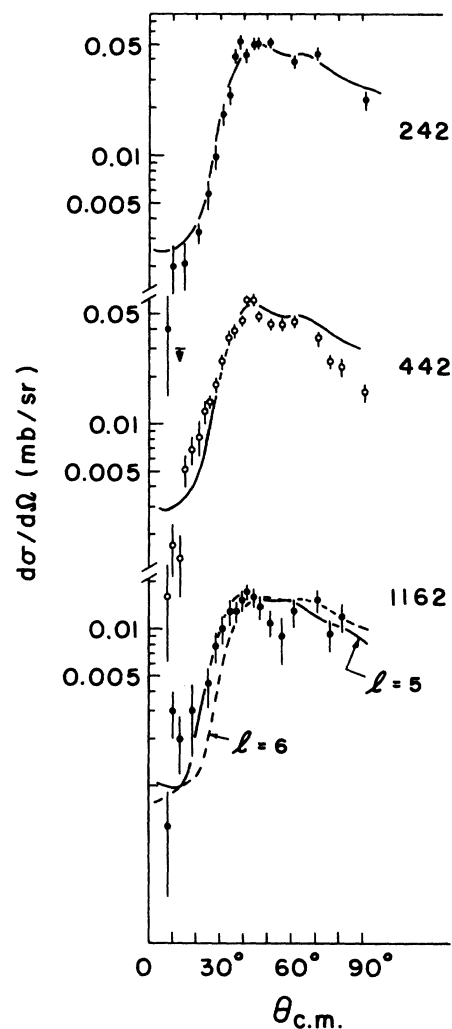


FIG. 7. Angular distributions for $l=5$ and $l=6$ transitions compared with DWBA calculations. The upper two distributions can only be fitted with $l=6$, while the transition to the state at 1162 keV is compared with $l=5$ and $l=6$ calculations. The arrow on the 12.5° data point for the transition to the 242-keV level indicates the upper bound to the cross section (1 standard deviation) determined from the experimental data. Where they are not shown, the error bars are smaller than the points.

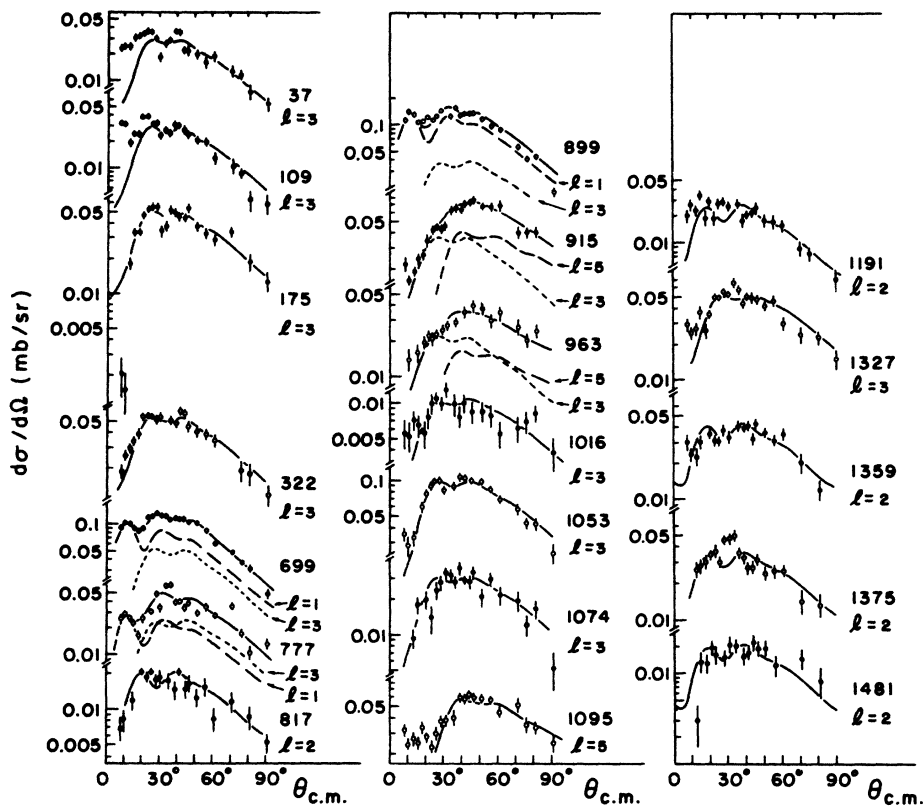


FIG. 8. Comparison of $^{169}\text{Tm}(d, t)^{168}\text{Tm}$ data with DWBA calculations for all remaining transitions. These are transitions of uncertain or mixed l -transfer values. Where a mixture of l values is able to fit an angular distribution, the individual DWBA predictions and the summed result are presented. Note that the $l=3$ predictions do not represent the data for the transitions to the 37- and 109-keV levels very well, as discussed in the text. Where they are not shown, the error bars are smaller than the points.

present experiment. Finally, strong $l=3$ transitions are seen to the $(3^-, 0)$ and $(4^-, 0)$ states at 344 and 380 keV, as predicted. All of the above assignments are in agreement with those proposed in Ref. 7. Notice, however, that there is also a strong $l=3$ transition to the state at 322 keV which might also be identified with the $(3^-, 0)$ state (Table I). The selection was made in Ref. 7 by analogy to the levels of ^{170}Tm for which the band assignments are known from γ -decay studies. The present experiment does not provide an independent test of this selection.

3. Other Levels

In addition to the $[521]_{\frac{1}{2}}^-$ Nilsson state, four other orbitals are expected to lead to observable negative-parity states with excitation energies below 1 MeV in ^{168}Tm . They are the $[521]_{\frac{3}{2}}^-$ and $[523]_{\frac{5}{2}}^-$ levels, which are hole states in ^{168}Tm , and also the $[512]_{\frac{5}{2}}^-$ and $[510]_{\frac{1}{2}}^-$ particle states. The $[512]_{\frac{5}{2}}^-$ orbital yields bands with $K^\pi = 2^-$ and 3^- . The states at 322 and 589 keV have previously

been identified⁷ as the $(3^-, 2)$ and $(4^-, 3)$ rotational states, respectively, and our data (Table I) lend support to these assignments. The rotational states resulting from the remaining Nilsson orbitals are very close in energy and strongly coupled by the Coriolis interaction. To complicate matters further, these states occur at or above the energy expected for the first vibrational excitation in this nucleus. In fact, both the $[521]_{\frac{3}{2}}^-$ and $[510]_{\frac{1}{2}}^-$ states have been interpreted in the neighboring ^{167}Er nucleus as members of complex bands involving 2^+ excitations.² For these reasons, no attempt was made in Ref. 7 to identify rotational bands above 600-keV excitation energy. The spin limits and parity assignments of Table I, however, provide new information which allows us to suggest tentative assignments for the majority of the negative-parity states below 900 keV.

The $[411]_{\frac{1}{2}}^+$ odd proton can couple to the $[521]_{\frac{3}{2}}^-$ neutron hole to produce two negative-parity bands with $K=1$ and $K=2$. Of these, the $K=1$ band is expected to occur at a lower excitation energy on the basis of the Gallagher-Moskowsky rule. The

states at 611, 661, 723, and 851 keV have the appropriate spins and parity to be the first four members of this $K^\pi = 1^-$ band, and in addition the level spacing is approximately as expected. The states at 699 and 915 keV then fitted in as the 2^- and 4^- members of the $K^\pi = 2^-$ band, respectively. There are, however, no unassigned levels in this energy region which qualify as the $(3^-, 2)$ state unless we assume that the state at 777 keV is an unresolved doublet, in which case the rotational level spacing is about as expected.

The $[523]_{\frac{5}{2}}^-$ neutron orbital leads to two bands having $K^\pi = 2^-$ and 3^- , with the 3^- band head expected to be lower. The states at 963 and 1095 keV have the correct spins and parity to be associated with the $(4^-, 3)$ and $(5^-, 3)$ rotational states. Under this assumption, the unperturbed $K^\pi = 3^-$ band head should lie at about 860 keV. There are several probable 3^- states just above 900 keV of excitation in ^{168}Tm which might be candidates for the 3^- band head if the band is strongly perturbed by the Coriolis interaction. On the other hand, the state at 851 keV which we have assigned as the $(4^-, 1)$ state based on the $[521]_{\frac{3}{2}}^-$ Nilsson orbital might also be the 3^- band head. Data from different reactions would perhaps be of some help in clearing up this point. The states at 899 and 1162 keV can most probably be identified with the $(2^-, 2)$ and $(5^-, 2)$ levels. There are several candidates for the 3^- and 4^- members of this band at about 950 and 1050 keV excitation.

Finally, the $[510]_{\frac{1}{2}}^-$ orbital can form $K^\pi = 0^-$ and 1^- bands which, like the bands based on the $[521]_{\frac{1}{2}}^-$ neutron state, can be expected to be strongly perturbed by the Coriolis interaction. This Nilsson orbital is a particle state in ^{168}Tm , but it has a large intrinsic strength so that at least the low angular momentum rotational levels should be observable in the (d, t) reaction. Possible candidates for the $(1^-, 0)$ and $(2^-, 0)$ rotational states are the levels at 789 and 833 keV, and the $l=1$ transition to the state at 882 keV might possibly be assigned to the $(2^-, 1)$ state.

New assignments for negative-parity states in ^{168}Tm suggested by the present experiment are summarized in Fig. 9. It should be emphasized that these proposed configurations are to be regarded as tentative because of the high degree of complexity of ^{168}Tm in this range of excitation energy. Other investigations, particularly of the γ -decay schemes of these states, would be most helpful in unraveling the spectrum.

In contrast to the complex negative-parity spectrum, there are only two positive-parity states in ^{168}Tm below 1100 keV other than the states originating from the $[633]_{\frac{7}{2}}^+$ Nilsson orbital which are discussed above. These states, at 766 and

817 keV, are at about the excitation energy expected for the $[642]_{\frac{5}{2}}^+$ bands ($K^\pi = 2^+$ and 3^+). The strong $l=4$ level at 766 keV is perhaps the $(4^+, 2)$ state.

Of more interest are the strong $l=0$ and $l=2$ transitions to states above 1100 keV. The Nilsson orbitals expected to contribute to states in this region are the $[400]_{\frac{1}{2}}^+$, $[600]_{\frac{1}{2}}^+$, $[402]_{\frac{3}{2}}^+$, and $[651]_{\frac{3}{2}}^+$ states, which should couple to eight states with $l=0$ transition strength. Four of these transitions are expected to be very strong, but the remaining four, those based on the $N=6$ Nilsson orbitals, should be several orders of magnitude weaker in the absence of Coriolis coupling. In actual fact we see four strong and four weak $l=0$ transitions. However, the weak transitions are less than an order of magnitude weaker than the strong transitions. It does not appear that the inclusion of Coriolis coupling alters the conclusion that the weak $l=0$ transitions are significantly stronger than expected by the standard Nilsson model with a harmonic-oscillator basis. Since this model tends to underestimate² the residual interaction between orbitals having $|\Delta N|=2$, the present data may provide additional information on the strength of the $|\Delta N|=2$ matrix elements.

B. Angular Distributions

As noted above, most of the angular distributions presented in this study exhibit clearly identifiable l -transfer patterns (Figs. 2-7). Only a minority of the experimental angular distributions cannot be acceptably fitted with a unique l value, and several of these are easily interpretable in terms of appropriate mixtures of l -transfer values (Fig. 8). There are, however, two exceptional angular distributions for transitions to states whose spectroscopic assignment is well known. These are the

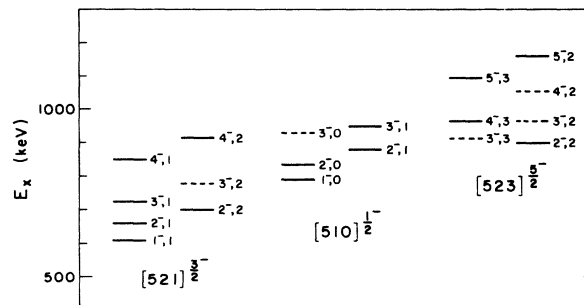


FIG. 9. New assignments for negative-parity states in ^{168}Tm suggested by the present experiment. The dashed levels are considered to be more uncertain, but it should be recognized that all of these proposed assignments are to be regarded as tentative because of the lack of other supporting evidence, particularly concerning the electromagnetic decay modes of the states in question.

angular distributions to the 37-keV ($2^-, 1$) state and the 109-keV ($3^-, 1$) state. In the former case, the Nilsson model predicts a mixed $l=3+1$ transition with the spectroscopic factor for $l=3$ about 2.5 times larger than for $l=1$. The experimental angular distribution (Fig. 8) suggests such an $l=3+1$ admixture but cannot in fact be fitted by any incoherent combination of $l=1$ and $l=3$ angular distributions. The transition to the 109-keV 3^- state should, of course, be pure $l=3$ in the DWBA whereas the observed shape (Fig. 8) bears little resemblance to the $l=3$ prediction. Indeed, it cannot be fitted by any incoherent linear combination of l values appropriate to a single state, and there is no evidence that this state is a doublet. Since the first excited state of the ^{169}Tm target is at 8 keV, it is reasonable to expect that these two angular distributions are evidence for the importance of higher-order effects in the (d, t) reaction on deformed nuclei. Similar effects seen in the (p, d) reaction on ^{171}Yb have been accounted for in terms of two-step processes.²³ It would be of interest to see if this is the case for the present reaction.

One additional point of interest regarding the experimental angular distributions is the apparent inability of the DWBA to fit the very strong diffraction structure characteristic of the $l=0$ angular distributions (Fig. 2). We have tried several different sets of optical-model parameters for both projectiles without successfully reproducing the experimental shapes. However, the $3s_{1/2}$ shell-model state (from which the $[400]_{1/2}^+$ Nilsson orbital is derived) is far below the 100-neutron

TABLE IV. Parameters used in the Coriolis-coupled Nilsson-model calculations for the negative-parity states of ^{168}Tm . The definitions of $\beta(0.3)$, $\mu(0.42)$, $\kappa(0.0637)$, a , and θ may be found in Ref. 2. Proton orbital (Ref. 2): $[411]_{1/2}^+$ $a=-0.88$.

Band-head energy (keV)	K^π	Neutron orbital	$\hbar^2/2\mathcal{J}$ (keV)
0	1^-	$[521]_{1/2}^-$	11.5
190	0^-	$[521]_{1/2}^-$	11.5
280	2^-	$[512]_{3/2}^-$	11.9
515	3^-	$[512]_{3/2}^-$	11.9
620	1^-	$[521]_{3/2}^-$	12.0
700	0^-	$[510]_{1/2}^-$	11.6
720	2^-	$[521]_{3/2}^-$	12.0
825	1^-	$[510]_{1/2}^-$	11.6
900	3^-	$[523]_{5/2}^-$	11.0
950	2^-	$[523]_{5/2}^-$	11.0

Fermi surface for any reasonable shell-model potential (i.e., ~ 50 MeV). Accordingly, the well depth necessary to generate form factors to bind these states at the empirical neutron separation energy is very shallow (<35 MeV). This problem arises in distorted-wave analyses of weak states in all nuclei and has been extensively discussed in the literature,²⁴ but it is particularly important in deformed nuclei^{16, 17} where even the strongest states may have binding energies very different from that of the centroid of the nearest appropriate shell-model state. It would be interesting to see if Rost's calculations,⁴ which use deformed single-particle wave functions, could reproduce the experimental $l=0$ diffraction pattern in more detail.

C. Spectroscopic Strengths

The spectroscopic intensities predicted by the Nilsson model for states in ^{168}Tm are subject to large inherent uncertainties due primarily to strong Coriolis coupling, particularly among the closely spaced negative-parity bands above 1 MeV of excitation. For this reason, we have made complete Coriolis-coupled Nilsson-model calculations only for the bands resulting from the $[521]_{1/2}^-$, $[512]_{3/2}^-$, $[521]_{3/2}^-$, $[523]_{5/2}^-$, and $[510]_{1/2}^-$ neutron orbitals. The remaining negative-parity bands were not included in the calculation, which was

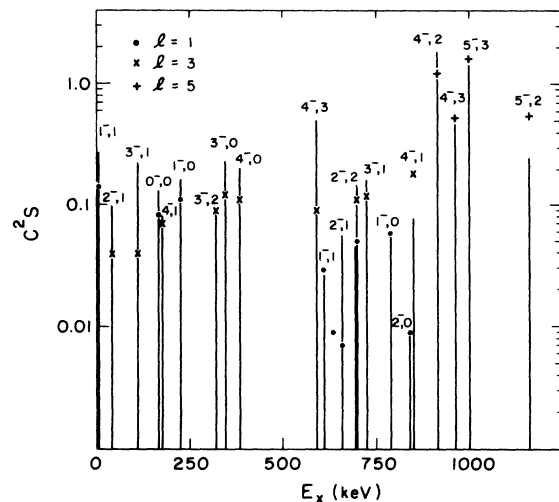


FIG. 10. Comparison of the experimental spectroscopic factors with Coriolis-coupled Nilsson-model calculations using the BANDMIX code. The dots are experimental values and the lines represent theoretical spectroscopic factors. The states are labeled with their spin and the K value of the band to which they belong. For certain strongly mixed states, the experimental and theoretical spectroscopic factors for both contributing l values are shown.

performed with the BANDMIX code,²⁵ using the parameters listed in Table IV. This code calculates expansion coefficients, C_{ji} , for unmixed Nilsson orbitals in a basis of spherical symmetry, allows the Coriolis interaction to mix Nilsson-model states, and so yields expansion coefficients, $C_{ji,\text{mixed}}$, for the final model states in a spherically symmetric basis. According to Satchler,²⁶ the squares of these expansion coefficients, $C_{ji,\text{mixed}}^2$, are to be compared with the spectroscopic factor, C^2S , measured in the single-nucleon-transfer reaction populating the state. The results of the BANDMIX calculation are shown in Fig. 10, in which the experimental and theoretical spectroscopic factors are compared for the known levels in these bands. It can be seen that the predicted spectroscopic factors are on the average about 50% larger than the experimentally measured values. This discrepancy in the absolute cross sections is somewhat larger than might be expected, but not seriously so considering the possible uncertainties in both the experimental⁵ and theoretical values.

After renormalizing the predicted spectroscopic factors to account for this discrepancy in the absolute cross sections, the agreement between experimental and theoretical spectroscopic factors is generally within $\pm 30\%$ except for a few noteworthy cases. In particular, the predicted spectroscopic factors for the $(2^-, 1)$ and $(3^-, 1)$ states at 37 and 109 keV are substantially higher than the experimental values. These same states also have anomalous angular distributions, which suggests that multiple excitation and direct processes may be interfering in the transitions to these levels. The $(1^-, 1)$ state at 0 keV is also weaker than predicted. It was suggested in Ref. 7 that the transition to this state is only about half as strong as expected on the basis of a comparison to the intensities of states resulting from the $[512]_{\frac{3}{2}}^-$ orbital in ^{170}Tm . The present results support this suggestion, but the magnitude of the discrepancy is uncertain because of the need to renormalize the predicted absolute spectroscopic factors to obtain over-all agreement with experiment. Fi-

nally, the $(2^-, 1)$ state at 661 keV is substantially weaker than expected, and its strength seems to be split over two $l=1$ states in this region of excitation energy. However, the interpretation of this discrepancy is not clear because of the large effects of Coriolis coupling on states above about 600 keV.

V. SUMMARY AND CONCLUSION

Excitation energies for 58 states in ^{168}Tm up to 1.5 MeV have been obtained to an accuracy of $\pm 0.15\%$, and the ground-state Q value for the $^{168}\text{Tm}(d, t)^{168}\text{Tm}$ reaction was found to be $Q_0 = -1775 \pm 6$ keV. The angular distributions for the transitions to most of these states were well described by the DWBA, and the deduced l -transfer values allowed the assignment of a narrow range of J^π values to these states independent of arguments based on Nilsson-model predictions of the transition strength. Angular distributions characteristic of all l values from 0 through 6 were observed. Spectroscopic factors for all of the observed transitions were computed, and the transition strengths to the low-lying negative-parity bands were compared to the Nilsson-model predictions.

The question of the adequacy of the DWBA in describing the present data is an important one, particularly in view of the fact that the first excited state of the ^{168}Tm target is at only 8 keV of excitation. Although most of the angular distributions appeared to be easily interpretable in terms of the DWBA, a few individual anomalous transitions to states which are otherwise well understood were observed. It would certainly be of some interest to see if these transitions could be accounted for in terms of collective or higher-order processes. Finally, one would like to investigate further the inability of the DWBA to reproduce the strong diffraction structure characteristic of all the $l=0$ transitions in the (d, t) reaction. This difficulty apparently also appears for (d, p) reactions²³ on strongly deformed nuclei; it may be partially due to the inconsistent use of spherical wave functions to describe these tightly bound states in deformed systems.

*Work supported by the National Science Foundation.

†Present address: Brookhaven National Laboratory, Upton, New York 11973.

¹O. Nathan and S. G. Nilsson, in *Alpha-, Beta-, and Gamma-Ray Spectroscopy*, edited by K. Siegbahn (North-Holland, Amsterdam, 1965), Vol. 1, p. 601.

²M. E. Bunker and C. W. Reich, *Rev. Mod. Phys.* **43**, 348 (1971).

³N. K. Glendenning and R. S. Mackintosh, *Nucl. Phys.* **A168**, 575 (1971); R. J. Ascutto and N. K. Glendenning,

Phys. Rev. **181**, 1396 (1969).

⁴E. Rost, *Phys. Rev.* **154**, 994 (1967).

⁵J. R. Erskine, *Phys. Rev. C* **5**, 959 (1972).

⁶See, for example, the references cited in Ref. 1.

⁷H. D. Jones and R. K. Shelton, *Ann. Phys. (N.Y.)* **63**, 28 (1971).

⁸J. V. Maher, J. J. Kolata, and R. Miller, *Bull. Am. Phys. Soc.* **16**, 514 (1971).

⁹Z. Preibisz and D. G. Burke, *Bull. Am. Phys. Soc.* **17**, 558 (1972).

¹⁰J. R. Comfort, ANL Physics Division Informal Report No. PHY-1970 B, 1970 (unpublished); and P. Spink and J. R. Erskine, ANL Physics Division Informal Report No. PHY-1965 B.

¹¹We are indebted to J. Childs for the use of his calibration code SPIRO (unpublished).

¹²C. M. Lederer, J. M. Hollander, and I. Perlman, *Table of Isotopes* (Wiley, New York, 1968), p. 397.

¹³A. H. Wapstra and N. B. Gove, Nucl. Data A9, 418 (1971).

¹⁴FORTTRAN-IV computer code DWUCK and instructions written by P. D. Kunz, University of Colorado (unpublished).

¹⁵F. G. Perey, in *Proceedings of the Rutherford Jubilee International Conference, Manchester, England, 1961*, edited by J. B. Birks (Heywood and Company, Ltd., London, England, 1962), p. 125; P. J. A. Buttle and L. J. B. Goldfarb, Proc. Phys. Soc. (Lond.) 83, 701 (1964); G. Bencze and J. Zimanyi, Phys. Lett. 9, 246 (1964); F. G. Perey and D. Saxon, Phys. Lett. 10, 107 (1964).

¹⁶N. Austern, Phys. Rev. 136, B1743 (1964).

¹⁷A. Prakash and N. Austern, Ann. Phys. (N.Y.) 51, 418 (1969).

¹⁸R. A. Harlan and R. K. Sheline, Phys. Rev. 168, 1373 (1968).

¹⁹J. V. Maher, J. J. Kolata, and J. L. Ricci, to be published; and J. L. Ricci, J. J. Kolata, R. W. Miller, and J. V. Maher, Bull. Am. Phys. Soc. 17, 558 (1972).

²⁰H. D. Jones, N. Onishi, T. Hess, and R. K. Sheline, Phys. Rev. C 3, 529 (1971).

²¹C. J. Gallagher and S. A. Moskowsky, Phys. Rev. 111, 1282 (1958).

²²R. K. Sheline *et al.*, Phys. Rev. 143, 857 (1966).

²³L. J. McVay, C. K. Bockelman, W. D. Callender, C. H. King, C. F. Maguire, and W. D. Metz, Bull. Am. Phys. Soc. 17, 486 (1972).

²⁴G. M. McAllen, W. T. Pinkston, and G. R. Satchler, Particles and Nuclei 1, 412 (1971) and references therein.

²⁵FORTTRAN-IV computer code written by J. R. Erskine (unpublished).

²⁶G. R. Satchler, Ann. Phys. (N.Y.) 3, 275 (1958).